Proceedings of the 40th Chinese Control Conference
July 26-28, 2021, Shanghai, China

Research on motion driving and tracking control of 3-DOF parallel stabilized platform

Shuo Jiang[1,2], Junzheng Wang[1,2], Shoukun Wang[1,2], Jiangbo Zhao[1,2]
1. School of Automation, Beijing Institute of Technology, Beijing, 100081, China
2. MIIT Key Laboratory of Servo Motion System Drive and Control, Beijing Institute of Technology, Beijing, 100081, China
E-mail: 15501212668@163.com

Abstract: The stabilized platform can keep the equipment's horizontal attitude above the carrier stable, provide a relative safe working environment, and possess the motion simulation function. Due to unknown and time-varying environmental information, the platform's stability control is susceptible to mechanical resonance, parameter gain chattering, and response lag. This paper proposes a three-degree-of-freedom (3-DOF) parallel stabilized platform and elaborates the design concept. A sliding mode variable structure controller (SMC) in single-cylinder based on the Lyapunov stability theory is designed, and we discuss the controller's adjustability. SMC improves system's control accuracy and environmental adaptability. Switching feedforward control method is applied to achieve horizontal postures stability. Attitude tracking experiments are carried out under different disturbance conditions to verify the feasibility of the algorithm.

Key Words: 3-DOF platform, Attitude tracking, Feedforward switching, Sliding mode control

1 Introduction

With the development of science and technology, vehicles, ships, and aircraft have been widely used. Attitudes above these vehicles will shift as the environment changes, and the equipment above them, such as seats, radars, and cameras, need to be stable. Simple cushioning devices can offset partial tilt but cannot cope with harsh conditions. Therefore, it's essential for the steady control of the stabilized platform under complex working conditions[1-2]. The stabilized platform is mainly used to isolate the carrier's movement and ensure that the equipment installed above has a stable working space under the action of external interference. It can be divided into series, parallel and hybrid types from structure, and its driving modes include electric, hydraulic, and pneumatic. Through the movement law opposite to disturbance, the platform is tilted relative to the carrier[3]. Fig.1 shows representative applications for stabilized platforms.

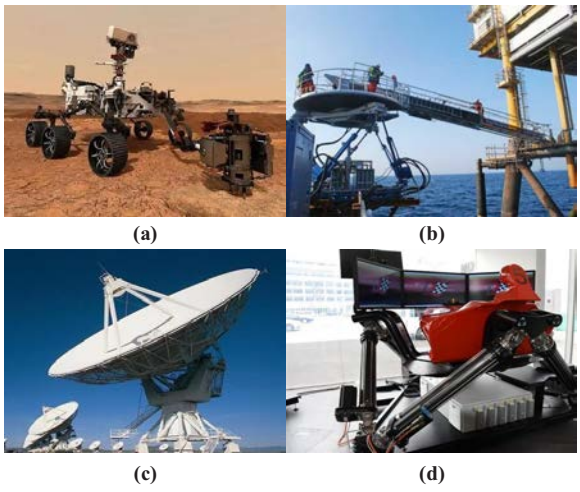

Fig. 1: Applications (a) Exploration (b) Offshore operation (c) Radar detection (d) VR driving

This work is supported by National Natural Science Foundation (NNSF) of China under Grant 61773060.

As the basic unit of stabilized platform's actuator, the servo-electric cylinder takes the advantages of compact structure, small inertia, fast response, and long-lasting. Some researchers proposed an event-triggered sampler based on the proportional differential form to improve electric cylinder's displacement control accuracy[4]. They designed a corresponding extended state observer to enhance the tracking performance. If we consider surface friction, it will involve load robust adaptive control[5]. The stabilized platform can detect disturbance signals through attitude sensor. However, gyroscope sensor always has an unavoidable delay or lag. Attitude signals can be corrected to a certain extent by feedforward control, which is a compensation mechanism. The disturbance will have a curative effect on the system, and steady-state error can be wholly eliminated in theory[6-7]. Attitude stability or tracking control requires hugely high requirements on sensor and algorithm tracking accuracy[8-9]. Panathula et al.[10] adopted high-order sliding mode variable structure robust control to achieve dynamic cascade compensation. A single-loop continuous attitude controller was designed to analyze system's actual stability margin to realize robustness. Scholars such as Brugarolas[11] have developed a feedforward-feedback attitude controller for the Mars thruster, which used the dead zone of PD or D control structure to save fuel while achieving rapid response to tracking tilt commands. Boehm J's research[12] was based on the dynamics control framework. It adopted a nonlinear control strategy to realize the six-degree-of-freedom tracking of propeller's remote-controlled aircraft attitude, speed, and speed set points.

2 System modeling

2.1 3-DOF stabilized platform

The experimental prototype (see Fig.2) consists of a 3-DOF parallel stabilized platform, an inertial load (buffer seat or iron block), a disturbance platform, and an inflatable device. Control system is constructed by a Linux-based industrial computer, which can collect position and force sensor feedback signals in real-time, process algorithms, and

send analog commands to PMSM drivers to drive electric cylinders. Communication system adopts a high-speed UDP communication protocol for data transmission. Compared with previously launched stabilized platforms, platform in Fig.2 can realize attitude stability control and 3-DOF motion tracking movements. It has improvements in mechanical structure, system hardware, and control algorithms. Fig.3 shows two versions of the experiment platforms. Compared with Version I, the mechanical structure of Version II is optimized that it's more stable and has more reasonable workspace. Verification experiments will be finished on both platforms.

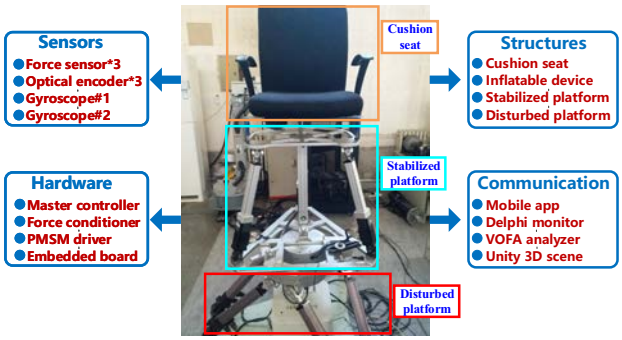

Fig. 2: 3-DOF stabilized platform

(a) **(b)**

Fig. 3: Stabilized platforms (a) Version I (b) Version II

2.2 Motion analysis

The kinematics of 3-DOF parallel stabilized platform includes forward solution from actuator's position to moving platform's posture and inverse solution from platform's given posture to elongation of cylinders. During the movement of the platform, Euler angles are used to describe the attitude of inertial coordinate system (roll and pitch angle), which can be defined as $q = \begin{bmatrix} \varphi_x & \varphi_y & \Delta z & +z_{init} \end{bmatrix}$ where z_{init} stands for the height between the moving and static platform when each electric cylinder locates at its initial position. We translate and rotate the coordinate axis according to the multi-rigid body rotation method in Cartesian coordinate system and define the rotation direction as $X-Y-Z$. Rotation matrix can be obtained by the right hand screw as

$$T = T(x, \varphi_x)T(y, \varphi_y) \tag{1}$$

Telescopic amount of each electric cylinder can be expressed as:

$$\Delta l_i = Tp_i - L_{\min}(i = 1, 2, 3) \tag{2}$$

where p_i is relative coordinate between upper and lower chassis. $L_{\min}$ is cylinder's initial length. Initial height of the platform is obtained by following formula

$$z_{init} = \sqrt{L_{\min}^2 - (R-r)^2} \tag{3}$$

where R and r stands for the radius of lower and upper chassis. Standard dynamic equation of the stabilized platform can be expressed as

$$\boldsymbol{M}(\boldsymbol{q})\ddot{\boldsymbol{q}} + \boldsymbol{C}(\boldsymbol{q}, \dot{\boldsymbol{q}})\dot{\boldsymbol{q}} + \boldsymbol{G}(\boldsymbol{q}) = \boldsymbol{\tau} \tag{4}$$

where $\boldsymbol{M}(\boldsymbol{q})$ is inertia matrix, $\boldsymbol{G}(\boldsymbol{q})$ is gravity term, $\boldsymbol{C}(\boldsymbol{q}, \dot{\boldsymbol{q}})\dot{\boldsymbol{q}}$ represents centripetal force or Coriolis force.

Since dynamic equation is a complex model with various variables and high nonlinearity, its accurate model is hard to get. We carry out co-simulation of kinematics and dynamics in Adams to verify structural design's rationality and in this way, we can obtain stabilized platform's workspace range.

3 Methods

3.1 Sliding mode robust controller design

Sliding mode variable structure control (SMC) method is essentially a special kind of nonlinear control. This controller's nonlinearity is manifested as its discontinuity. The system's structure is not fixed, and it may change continuously according to the current state in dynamic process. System moves according to state trajectory of predetermined sliding mode. SMC takes the advantages of fast response, insensitive to parameter changes or disturbances, no need for system online identification, and simple physical realization. The design of SMC based on exponential reaching law is shown in Fig.4.

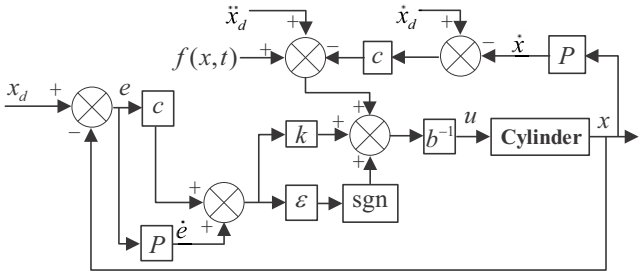

Fig. 4: Sliding mode controller design in single electric cylinder

The equivalent transmission model of servo electric cylinder can be expressed as:

$$\begin{cases} \ddot{x}_d = -f(x,t) + bu(t) \\ f(x,t) \propto J\dot{x}, b > 0 \end{cases} \tag{5}$$

where x_d is cylinder's given position, x is feedback position. b and J depends on PMSM, which can be obtained by manual or parameter identification.

Cylinder's displacement and speed tracking error together with sliding mode function are designed as follows:

$$\begin{cases} e(t) = x_d(t) - x(t) \\ \dot{e}(t) = \dot{x}_d(t) - \dot{x}(t) \\ s(t) = ce(t) + \dot{e}(t) \end{cases} \tag{6}$$

where $c > 0$, c must satisfies Huiwitz condition:

$$\begin{cases} \dot{x} = Ax + bu \\ s(x) = C^T x = \sum_{i=1}^{n-1} c_i x_i + x_n \end{cases} \tag{7}$$

For linearized systems, $p^{n-1} + c_{n-1}p^{n-2} + \cdots c_2 p + c_1$ is Huiwitz. p is laplace operator. Then we have

$$\begin{aligned} &\dot{s}(t) = c(\dot{x}_d(t) - \dot{x}(t)) + (\ddot{x}_d(t) - \ddot{x}(t)) \\ &= c(\dot{x}_d(t) - \dot{x}(t)) + \ddot{x}_d(t) + f(x,t) - bu(t) \end{aligned} \tag{8}$$

When state trajectory reaches sliding mode surface, it traverses back and forth on both sides of the sliding mode balance surface, which may cause vibration. Robust control means that the control system maintains the characteristics of stability under specific parameter perturbations, and the application of sliding mode approaching law can eliminate chattering.

$$\dot{s}(t) = -\varepsilon \operatorname{sgn} s - ks(\varepsilon > 0, k > 0) \tag{9}$$

We define the Lyapunov function as:

$$\begin{cases} V = \frac{1}{2}s^2 \\ \dot{V} = s\dot{s} \le -\varepsilon |s| = ks^2 \le 0 \\ V \le e^{-\frac{k}{2}(t-t_0)} V(t_0) \end{cases} \tag{10}$$

where $\dot{s}(t) = -ks$ is the exponential approaching term, which determines system's convergence speed, ensuring that when s is large, system can approach sliding mode dynamics with fast speed. $\dot{s}(t) = -\varepsilon \mathrm{sgn} s$ is the equivalent velocity approaching term which eusures that when s approaches zero, approach speed is not zero.

System can reach sliding surface within a finite time. In the exponential approach law, in order to ensure rapid approach while reducing vibration, we should increase k while decreasing ε.

Combining equation 8, 9 and 10, we can obtain control law as:

$$c(\dot{x}_d(t) - \dot{x}(t)) + \ddot{x}_d(t) + f(x,t) - bu(t) = -\varepsilon \mathrm{sgn} s - ks \tag{11}$$

PMSM driver analog input value can be experessed as:

$$u(t) = b^{-1}(\varepsilon \mathrm{sgn} s + ks + c(\dot{x}_d(t) - \dot{x}(t)) + \ddot{x}_d(t) + f(x,t)) \tag{12}$$

Furthermore, let's discuss the practicability of a robust adaptive SMC considering the friction model. This improved controller can modify electric cylinder's expansion contraction characteristics in real-time to be adaptive to dynamic characteristics of disturbance. Adaptive adjustment stragety is required to obtain the estimated value of motor's moment of inertia.

Control law satisfies:

$$u(t) = \hat{J}(\ddot{x}_d(t) - c\dot{e}) - ks - \eta \mathrm{sgn}(s) \tag{13}$$

The adaptive law can be obtained as:

$$\frac{d\hat{J}}{dt} = -\gamma s(\ddot{x}_d - c\dot{e}) \tag{14}$$

It should be noticed that this improved controller must be executed in the torque mode of PMSM driver. The state space equation is

$$\begin{cases} \ddot{x}_d = u(t) + \Delta \\ \Delta = F_c \mathrm{sgn}(\dot{x}) + b_c \dot{x} \end{cases} \tag{15}$$

where Δ is viscous friction model. F_c and b_c is empirical estimation parameters, η and γ can be artificially determined.

3.2 Feedforward switching control strategy

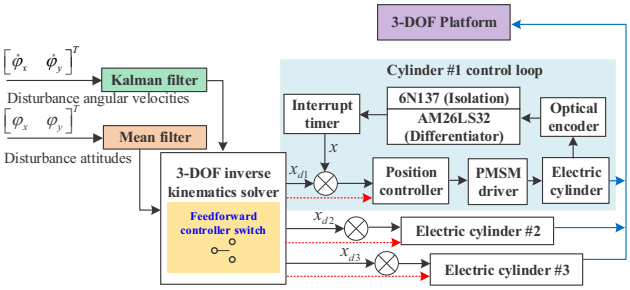

Fig. 5: Feedforward switching control strategy

In this section, a feedforward-feedback switching control strategy (see Fig.5) is put forward to solve the attitude stability and tracking control problems of 3-DOF platform. The main issues are as follows:

- (a) Generalized hardware performance: As the working mode of attitude sensor (gyroscope) under Linux is query rather than interrupt, the control cycle sometimes is long (15ms) and unstable (see Fig.6), which causes chattering and crawling.
- (b) System error: Due to platform's mechanical clearance of Hooke joints, kinematics calculation error exists, which may cause platform's horizontal vibration.
- (c) Singal lagging and chattering (see Fig.7): Gyroscope's dynamic precision affects stability tracking control performance. Angular velocities obtained by direct differentiation or gyroscope have lag and jitter.

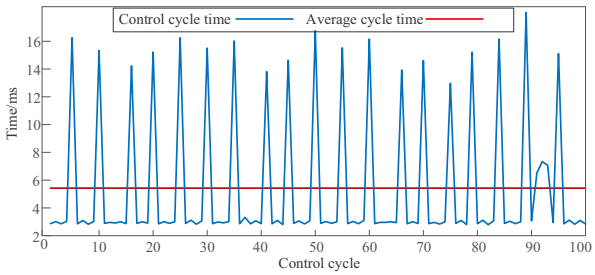

Fig. 6: Issue (a) Unstable control cycle

To solve issue (a), the serial thread mode is optimized and it reduces system's average control cycle within 3ms. Then we use laser light pre-calibrate strategy (see Fig.8) to locate the surrounding point to eliminate gaps in issue (b).

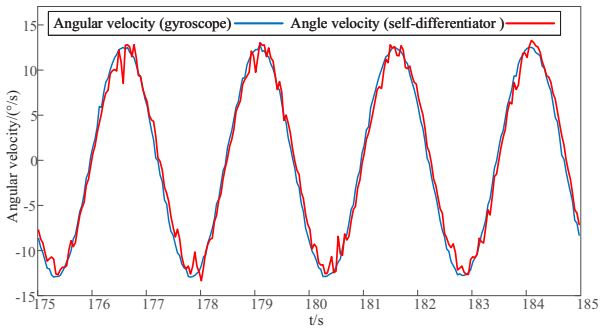

Fig. 7: Issue (c) Singal lagging and chattering

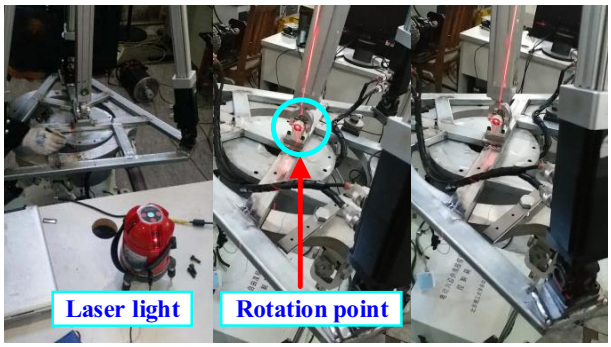

Fig. 8: Laser light pre-calibrate strategy

To realize stable attitude tracking, we first apply Kalman filter based full-range fast differentiator to angular velocity signals of the gyroscope (MTi-300). The empirical eqaution group is listed as follows:

$$\begin{cases} \hat{X}(k+1|k) = \Phi\hat{X}(k|k) \\ \hat{X}(k+1|k+1) = \hat{X}(k+1|k) + K(k+1)\varepsilon(k+1) \\ \varepsilon(k+1) = Y(k+1) - H\hat{X}(k+1|k) \\ K(k+1) = P(k+1|k)H^T[HP(k+1|k)H^T + R]^{-1} \\ P(k+1|k) = \Phi P(k|k)\Phi^T + \Gamma Q\Gamma^T \\ P(k+1|k+1) = [I_n - K(k+1)H]P(k+1|k) \end{cases} \tag{16}$$

where $\hat{X}(k+1|k)$ is the estimated value of one step predicted angular velocity state. $\hat{X}(k+1|k+1)$ is state update matrix. $K(k+1)$ stands for filter gain matrix. $P(k+1|k)$ is one-step prediction covariance matrix. Covariance matrix can be updated as $P(k+1|k+1)$.

Since angle singals are smoother than angular velocity signals, we only use mean filter to deal with angle signals. The feedforward-feedback switching control stragtegy includes two kind of feedforward controllers. When roll or pitch disturbance angle is large, the feedforward fomula can be expressed as:

$$\begin{cases} \varphi_x = \varphi_x + \lambda_1\dot{\varphi}_x \\ \varphi_y = \varphi_y + \lambda_2\dot{\varphi}_y \end{cases} \tag{17}$$

It can be viewed as extra input of given angle. This strategy is useful for single-axis attitude tracking control. However, when we simualte complex terrain, both roll and pitch angle cannot be ignored, the feedforward formula can be obtained as:

$$\begin{cases} u_i(t) = u_i(t) + \lambda_3 v_i(t) \\ v_i(t) = |B_i - T_i|' \end{cases} \tag{18}$$

where $u_i(t)$ is PMSM driver analog input. $v_i(t)$ stands for electric cylinder's velocity, which can be obtained by the coordinates B_i and T_i in moving platform and static platform. This formula also depends on the angular velocity. λ_1, λ_2 and λ_3 are feedforward coefficients.

4 Experiment analysis

4.1 Single-cylinder position tracking experiments

The experiments are performed on the device shown in Fig.1. First, we carry out single cylinder position tracking control experiments with 10kg load. PD and SMC controllers are applied respectively to drive the cylinder to follow a sinusoidal signal (Vpp=60mm, Fre=0.4Hz). PD regulator is suitable for large delay link in servo system. When the adjustment deviation changes rapidly, the adjustment amount can be strengthened in the shortest time with adjustment static error. It's easy to see from Fig.9 that PD may cause adjustable static error, which is only suitable for extensive delay links. SMC works better than PD controller.

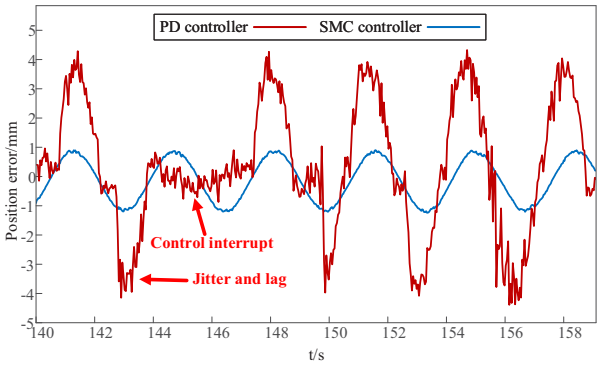

Fig. 9: Single cylinder position tracking experimental results under SMC and PD controller

Then, Fig.10 and Fig.11 shows position tracking phase locus under different SMC exponential and equal-velocity approach terms. Error decreases when k increases, and cylinder moves to SMC stable plane faster when ε decreases. But larger k may cause an initial velocity step, which is harmful to PMSM. The experimental results are in agreement with the theoretical analysis.

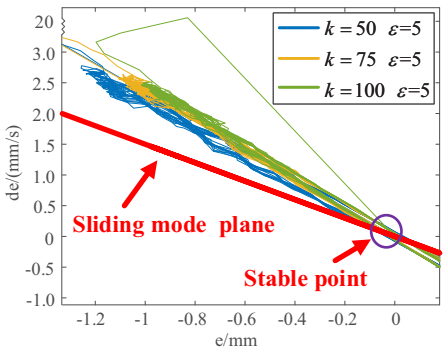

Fig. 10: Sliding mode phase locus experimental results under different gain parameters

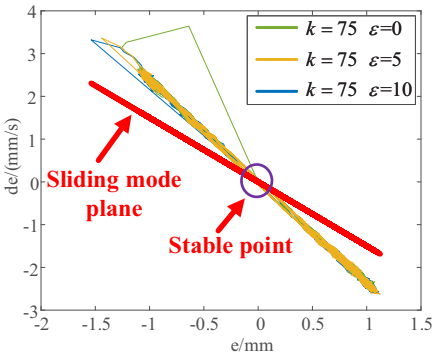

Fig. 11: Sliding mode phase locus experimental results under different ε

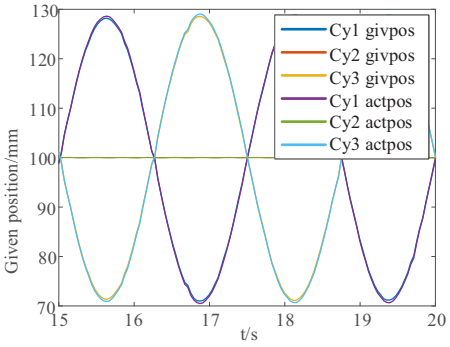

Fig. 14: Position tracking experimental results: Given position of each electric cylinder

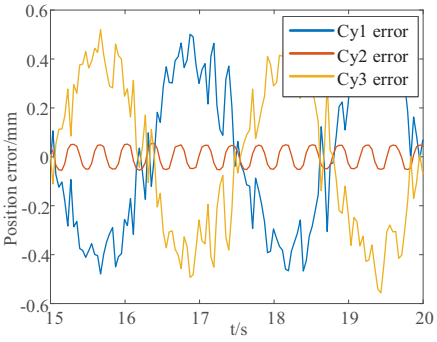

Fig. 15: Position tracking experimental results: Position error of each electric cylinder

4.2 Motion tracking experiments

In Fig.12, a sinusoidal roll motion (Vpp=10° Fre=0.4Hz) is performed, and it can be seen from Fig.13 that the tracking feedback error is limited within 0.2° that tracking efficiency reaches 96%. After many rounds of testing without this strategy, the feedback error rised to 1.6° that tracking efficiency falls down to only 68%. Sometimes the system cannot response to relatively high frequency working condition without feedforward strategy. Fig.14 and Fig.15 show the tracking experimental results that each cylinder's position error can be limited to 0.5mm.

Fig. 12: Motion control experiments (roll axis tracking)

Fig. 16: Compound motion control experiments

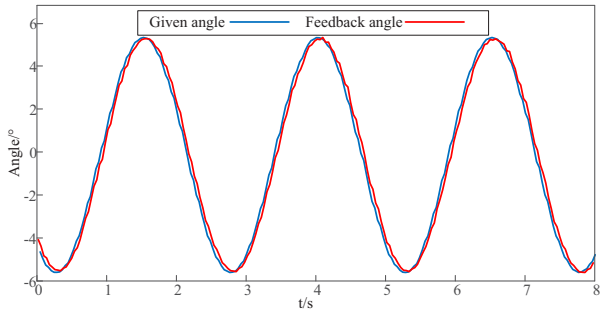

Fig. 13: Attitude tracking experimental results Vpp=10° Fre=0.4Hz

3-DOF compound motion control experiments (see Fig.16) verify the rationality of structural design. When pitch motion reaches limit, there's still at least 5° workspace left for roll motion and about 30mm left for the right and left-side cylinders. Experimental results are consistent with the theoretical calculation.

4.3 Attitude stability control experiments

Finally, attitude stability control experiments are carried out under roll and pitch disturbances (see Fig.17). We set up disturbance: sinusoidal roll signal (Vpp=10°, Fre=0.5Hz), sinusoidal pitch signal (Vpp=8°, Fre=0.6Hz). The disturbance signal can be finished by a 6-DOF large Stewart platform under the stabilized platform.

To analyse the stabilized efficiency from the experimental results, it can be seen from Fig.18 that the roll angle on upper chassis can be stabilized within ±0.5°. Stabilized efficiency is 90% (see Fig.18 (a)). Simultaneously, the pitch angle on top of the platform is limited to ±0.3° with high stabilized efficiency of 92.5% (see Fig.18 (b)).

In all, this stabilized platform can realize not only multi-

DOF motion movements but can also be used as a stabilized device to eliminate disturbance. In this paper, we don't care about vertical stability. Different from no-load condition, self-disturbance of coupling load force problem may affect attitude stability control, and it will be stdudied in the future.

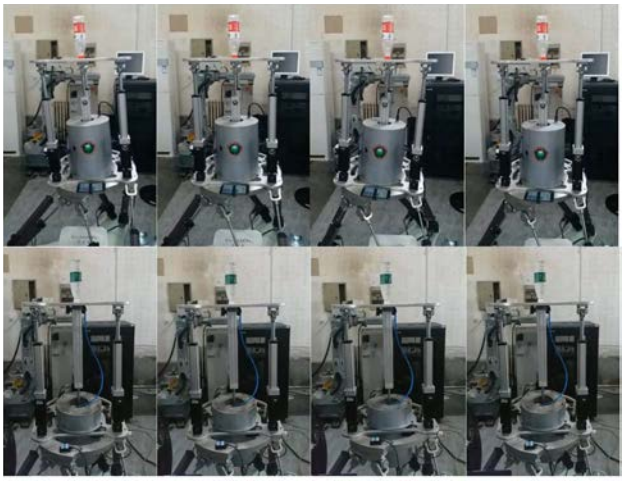

Fig. 17: Attitude stability control experiments

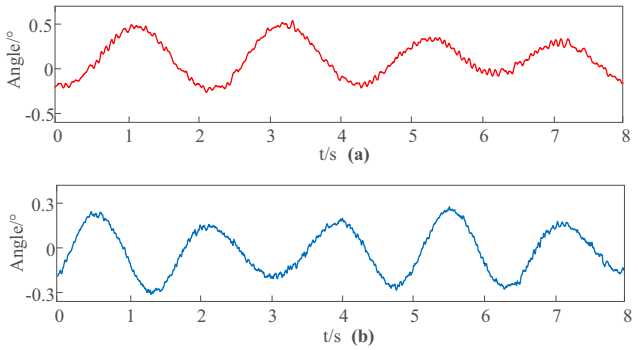

Fig. 18: Attitude stability experimental results
(a) Roll angle on upper chassis (b) Pitch angle on upper chassis

5 Conclusion

This paper proposes an electric parallel three-degree-of-freedom (3-DOF) stabilized platform. First, the platform's kinematics and dynamics models are built to provide research basis for motion control. Then, the single-cylinder sliding mode controller (SMC) is designed to improve response tracking accuracy, and we discuss the parameter adaptive adjustment strategy. A feedforward-feedback switching method is put forward to achieve roll, pitch, and compound attitude stability tracking control. Experimental results verify the correctness of proposed algorithm and structure. This platform can automatically detect disturbance, calculate lifting displacement of each electric cylinder, and realize key communication with the host computer. In all, the stabilized platform integrates 3-DOF motion movements together with attitude stability control function, which has a wide range of application prospects.

References

[1] J. M. Hilkert, "Inertially stabilized platform technology concepts and principles," *IEEE control systems*, vol. 28, no. 1, pp. 26–46, 2008.

[2] Z. Chen, S. Wang, J. Wang, K. Xu, T. Lei, H. Zhang, X. Wang, D. Liu, and J. Si, "Control strategy of stable walking for a hexapod wheel-legged robot," *ISA Transactions*, 2020.

[3] V. Z. Jr, F. R. Driscoll, T. S. Vanzwieten, and S. P. Marikle, "Development of an adaptive disturbance rejection system for the rapidly deployable stable platform-part 1: Mathematical modeling and open loop response," *Ocean Engineering*, vol. 37, no. 8-9, pp. 833–846, 2010.

[4] D. Liu, J. Wang, S. Wang, and D. Shi, "Active disturbance rejection control for electric cylinders with pd-type event-triggering condition," *Control Engineering Practice*, vol. 100, p. 104448, 2020.

[5] M. Fakoor, C. Volos, P. Nikpey, H. Jahanshahi, and N. N. Sari, "Optimal robust control approaches for a geostationary satellite attitude control," *International Journal of Automation and Control*, vol. 14, no. 3, p. 333, 2020.

[6] D. Lee and H. Leeghim, "Reaction wheel fault-tolerant finite-time control for spacecraft attitude tracking without unwinding," *International Journal of Robust and Nonlinear Control*, no. 5, 2020.

[7] C. Wang, L. Guo, C. Wen, Q. Hu, and J. Qiao, "Event-triggered adaptive attitude tracking control for spacecraft with unknown actuator faults," *IEEE Transactions on Industrial Electronics*, pp. 1–1, 2019.

[8] J. Li, J. Wang, H. Peng, L. Zhang, and H. Su, "Neural fuzzy approximation enhanced autonomous tracking control of the wheel-legged robot under uncertain physical interaction," *Neurocomputing*, vol. 410, 2020.

[9] L. Yu, G. He, S. Zhao, X. Wang, and L. Shen, "Immersion and invariance-based sliding mode attitude control of tilt trirotor uav in helicopter mode," *International Journal of Control, Automation and Systems*, pp. 1–14, 2020.

[10] C. B. Panathula, A. Rosales, Y. B. Shtessel, and L. M. Fridman, "Closing gaps for aircraft attitude higher order sliding mode control certification via practical stability margins identification," *IEEE Transactions on Control Systems Technology*, pp. 1–15, 2017.

[11] P. Brugarolas, A. S. Martin, and E. Wong, "Attitude controller for the atmospheric entry of the mars science laboratory," in *Aiaa Guidance, Navigation & Control Conference & Exhibit*, 2013.

[12] S. C. Boehm J, Berkenpas E, "Feedback-linearizing control for velocity and attitude tracking of an rov with thruster dynamics containing input dead zones," in *American Control Conference (ACC)*, 2019.